applied optics

Characterization of e-beam evaporated Ge, YbF_3, ZnS, and LaF_3 thin films for laser-oriented coatings

Tatiana Amotchkina,[1,*] Michael Trubetskov,[2] Daniel Hahner,[1] and Vladimir Pervak[1]

[1]Ludwig-Maximilians-Universität München, Am Coulombwall 1, 85748 Garching, Germany
[2]Max-Planck-Institut für Quantenoptik, Hans-Kopfermann-Str. 1, 85748 Garching, Germany
*Corresponding author: Tatiana. Amotchkina@physik.uni-muenchen.de

Received 13 September 2019; revised 25 October 2019; accepted 29 October 2019; posted 29 October 2019 (Doc. ID 378017); published 2 December 2019

Thin films of Ge, ZnS, YbF_3, and LaF_3 produced using e-beam evaporation on ZnSe and Ge substrates were characterized in the range of 0.4–12 μm. It was found that the Sellmeier model provides the best fit for refractive indices of ZnSe substrate, ZnS, and LaF_3 films; the Cauchy model provides the best fit for YbF_3 film. Optical constants of Ge substrate and Ge film as well as extinction coefficients of ZnS, YbF_3, LaF_3, and ZnSe substrate are presented in the frame of a non-parametric model. For the extinction coefficient of ZnS, the exponential model is applicable. Stresses in Ge, ZnS, YbF_3, and LaF_3 were estimated equal to (−50) MPa, (−400) MPa, 140 MPa, and 380 MPa, respectively. The surface roughness does not exceed 5 nm for all films and substrates.

https://doi.org/10.1364/AO.59.000A40

1. INTRODUCTION

Today, a number of mid-infrared (MIR) laser applications are being developed [1]. Among them are laser systems supporting biological, chemical, and bio-medical studies harnessing MIR radiation in the region from 3 to 15 μm, where most organic molecules exhibit fundamental vibrational and rotational modes [2]. Multilayer optical coatings, being key elements in the new laser systems and their applications, are challenged by growing demands on the spectral and phase performance, low losses, thermal stability, spectral stability, low absorption in water bands, and mechanical properties. The films with low losses are required not to lose the pulse energy; low stresses in films prevent deformation of the optical elements and distortion of the laser beams. Although conventional MIR multilayer optical components (filters, antireflection coatings) have been manufactured for many years [3], broadband MIR laser-related coatings have not been investigated. The most important MIR laser-related optical components are dispersive mirrors very often exhibiting positive group delay dispersion [4,5]. Due to the development of newly emerging broadband, temporally coherent MIR sources [6–10], dispersive optics operating in a much broader spectral range is required. Enhancement cavity applications require MIR mirrors exhibiting high reflectance, a controlled level of transmittance, and flat group delay dispersion [11]. Some laser applications demand NIR–MIR coatings operating simultaneously in the near-infrared (NIR) and in the MIR spectral ranges [12]. MIR antireflection coatings are required for the development of quantum cascade lasers [13].

One of the important prerequisites to producing high-quality laser-related optical coatings is knowledge of accurate optical constants of the layer materials and substrates as well as the mechanical/environmental properties of the layers. It is important to have reliable dispersion of refractive indices and extinction coefficients in broadband spectral ranges from 0.4 μm to 12–15 μm. In the present work, single layers of Ge, ZnS, YbF_3, and LaF_3 thin-film materials, and two substrates, ZnSe and Ge, are studied. There are a few publications devoted to various aspects of optical and non-optical characterization of some of these materials. Determination of the optical constants of Ge films on CaF_2 substrate in the broadband spectral range from 0.4 μm to 25 μm using the multi-oscillator model was reported in [14]. Optical constants of evaporated Ge films in the range 0.2–2 μm are published in [15]; the refractive index values are, however, quite low. The effects of evaporation parameters on the structural and electrical properties of Ge films were studied in [16]. A review of publications on Ge films and bulk Ge can be found in [17]. ZnS was a very well-known high-index material for VIS–MIR applications [18], which was later replaced in the VIS–NIR by TiO_2. Today, its importance

for MIR and NIR–MIR coatings is growing, since the thin-film material can be used as a high-index material in the combination of ZnS/YbF_3 [12] or ZnS/YF_3 [13], or as a low-index material in the well-established combination with Ge [4]. It is mentioned in Ref. [19] that the optical constants of deposited ZnS are strongly dependent on the deposition parameters. The dispersion behavior of ZnS optical constants can be found, for example, in [20,21]. The influence of the substrate temperature on the condensation and properties of ZnS films was studied in [22]. It should be noted that the well-known Ge/ZnS combination is not always suitable for modern laser-oriented coatings since the refractive index ratio is not high enough to provide sophisticated spectral characteristics in ultra-broadband spectral ranges (see, for example, the recent paper [12]). In particular, this pair cannot provide good dispersive mirror designs in the ranges essentially broader than in Ref. [4], for example, the 6–12 μm range. Also, Ge/ZnS coatings absorb up to 2 μm and cannot be used for NIR–MIR coatings in the case in which the transmittance in the VIS–NIR range should be non-zero. For such coatings, ZnS/YbF_3 or ZnS/LaF_3 combinations can be used. The YbF_3 thin-film material with refractive index ∼1.5 is relatively new, and it replaces highly toxic radioactive ThF_4, which was widely used earlier as a low-index material in the MIR range [18]. In [23], YbF_3 thin films were prepared through conventional thermal evaporation and ion beam-assisted deposition and characterized based on ellipsometric data in the range of 0.4–2.2 μm. In [24], YbF_3 films were prepared through ion-assisted deposition; the dependency of their mechanical properties on deposition conditions was investigated. In [25], optical constants of YbF_3 and LaF_3 films deposited at 200°C were determined in the range of 2–20 μm using the Lorentz model. Refractive index and extinction coefficient values in the range of 0.6–12 μm of a YbF_3 film evaporated at 250° as well as the results of the durability tests were reported in [26]. The LaF_3 films have been well studied, but mainly in the ultraviolet and visible (VIS) ranges (see, for example, [27,28]). In [29], evaporation procedures were established for some fluorides, among them LaF_3, and optical constants at two wavelength points of 8 μm and 10 μm were reported.

Characterization of MIR single layers is an extensive topic as the dependence of optical constants on deposition parameters [19] and the optical and mechanical properties of MIR films can be dependent on some other factors. In particular, as some MIR substrates (for example, ZnSe, KBr, ZnS, and partially Ge) transmit heat radiation in the range of 10–15 μm, they stay cooler than is indicated by the thermocouple in the vacuum chamber. The deviations of the substrate temperature may cause (i) dependence of the optical constants of layers on the substrate choice and (ii) dependence of the optical parameters on the layer thickness coordinate.

The primary goal of this study is to present reliable broadband wavelength dependencies of the optical constants of four MIR thin-film materials suitable for design and production of the laser-related MIR coatings operating in VIS–NIR–MIR spectral regions. The secondary goal of the present work is to demonstrate the characterization process of MIR films including choice of dispersion model, verification of the results, and estimation of stresses.

2. EXPERIMENTAL SAMPLES, MEASUREMENT DATA, AND OPTICAL CHARACTERIZATION

The summary of the experimental samples is presented in Table 1. All thin-film samples were produced by electron-beam evaporation at the SyrusPro 710 deposition plant (Bühler Leybold Optics). The substrate temperature was 120°C, which is lower than in references listed in Section 1. The vacuum system was pumped down to 10^{-6} mbar before the process. The film thicknesses were chosen as typical quarter-wave thicknesses in the range of 3–15 μm. The cleaned substrates directly from the supplier were not pretreated before the deposition. Reflectance and transmittance curves in the VIS–NIR range of 0.4–2.6 μm were measured using a Lambda 950 spectrophtometer (Perkin Elmer) with a wavelength step of 2 nm. Transmittance and reflectance data in the range of 2.6–25 μm were taken using the Fourier transform infrared spectrometer Vertex 70 (Bruker Optics GmbH). Total losses in the thin-film samples $TL(\lambda) = 100\% - T(\lambda) - R(\lambda)$ allowed one to find spectral ranges where the sample is non-absorbing, slightly

Table 1. Summary of Experimental Samples

Sample	Film	Substrate	Planned/Actual Thickness	Dispersion Model	
				$n(\lambda)$	$k(\lambda)$
ZnSe-sub	–	ZnSe, 1 mm	–	Sellmeier	Non-parametric
Ge-sub	–	Ge, 6.35 mm	–	Non-parametric	Non-parametric
ZnS-Ge	ZnS	Ge, 3 mm	1 μm/1.008 μm	Sellmeier	Exponential
ZnS-B260		B260, 1mm	1 μm/0.997 μm		–
YbF3-ZnSe-1	YbF_3	ZnSe, 1 mm	2 μm/1.95 μm	Cauchy	Non-parametric
YbF3-ZnSe-2			0.8 μm/0.795 μm	–	–
YbF3-B260		B260, 1 mm			
LaF$_3$-ZnSe-1	LaF_3	ZnSe, 1 mm	1.3 μm/1.368 μm	Sellmeier	Non-parametric
LaF$_3$-ZnSe-2			0.65 μm/0.672 μm	–	–
LaF3-B260		B260, 1 mm			
Ge-ZnSe-1	Ge	ZnSe, 1 mm	0.45 μm/0.42 μm	Non-parametric	Non-parametric
Ge-ZnSe-2			2.9 μm/0.849 μm		

absorbing, or significantly absorbing and to choose reliable dispersion models.

In the course of the characterization process, dispersion curves $n(\lambda)$, $k(\lambda)$ of the produced MIR films and substrates were described by model wavelength dependencies. The model parameters were found by the minimization of the discrepancy function judging the closeness between the model $S(\mathbf{X}; \lambda_j)$ and the measured $\hat{S}(\lambda_j)$ spectral characteristics on the wavelength grid $\{\lambda_j\}$, $j = 1, \ldots, L$ in the spectral range of interest:

$$DF^2 = \frac{1}{L}\sum_{j=1}^{L}\left(S\left(\mathbf{X}; \lambda_j\right) - \hat{S}\left(\lambda_j\right)\right)^2 \to \min, \quad (1)$$

where $\mathbf{X}$ is the vector including model parameters and the layer thickness d.

In the broadband spectral ranges including VIS, NIR, and MIR, it is not always possible to describe optical constants in the frame of simple parametric dispersion models such as three-parametric Cauchy or the more complicated seven-parametric Sellmeier model. In such cases, a non-parametric approach can be applied [30,31], where the discrepancy function is written in the following way:

$$DF^2 = \sum_{j=1}^{L}\left[S\left(n\left(\lambda_j\right), k\left(\lambda_j\right), d; \lambda_j\right) - \hat{S}\left(\lambda_j\right)\right]^2 + \alpha_1\sum_{j=1}^{L}\left[n''\left(\lambda_j\right)\right]^2 + \alpha_2\sum_{j=1}^{L}\left[k''\left(\lambda_j\right)\right]^2 \to \min. \quad (2)$$

Here, $n''(\lambda)$ and $k''(\lambda)$ denote finite-difference second-order derivatives of the refractive index and extinction coefficient, respectively. The second and the third terms in Eq. (2) specify the additional demands on smoothness of the $n(\lambda)$ and $k(\lambda)$ functions; the parameters α_1 and α_2 are weight factors balancing the smoothness and fitting demands. Characterization in the present work was performed using OptiLayer Thin Film software [32].

3. CHARACTERIZATION OF ZnSe AND Ge SUBSTRATES

Characterization of thin films typically requires determination of the optical constants of uncoated substrates. The refractive index of ZnSe substrate can be described by the Sellmeier model:

$$n^2(\lambda) = A_0 + \frac{A_1\lambda^2}{\lambda^2 - A_2} + \frac{A_3\lambda^2}{\lambda^2 - A_4} + \frac{A_5\lambda^2}{\lambda^2 - A_6}. \quad (3)$$

The dispersion behavior of the extinction coefficient of ZnSe substrate was specified by a smooth dependence $k(\lambda)$. Figure 1(a) demonstrates the determined optical constants of the ZnSe substrate and its remarkable agreement with the reference data [33,34]. Achieved fitting of the experimental data by model data is presented in Fig. 1(b). The Sellmeier coefficients were found equal to $A_0 = 0.310182$, $A_1 = 4.855169$, $A_2 = 0.056359$, $A_3 = 0.673922$, $A_4 = 0.056336$, $A_5 = 2, 481890$, and $A_6 = 2222.114$; all coefficients here and below correspond to the wavelength expressed in micrometers.

In the case of Ge substrate characterization, simple parametric models are not suitable, and more complicated multi-oscillator models are required [14]. It was shown in our previous work [35] that the multi-oscillator approach and the non-parametric algorithm [Eq. (2)] exhibit very close results. Ge substrate was characterized in the range of 0.4–11.2 μm using the non-parametric algorithm. Then, in order to verify the reliability of the obtained results, the refractive index of Ge substrate was determined in the range of transparency of 2–11.2 μm with the help of the well-known Cauchy model:

$$n(\lambda) = A_0 + \frac{A_1}{\lambda^2} + \frac{A_2}{\lambda^4}, \quad (4)$$

where A_0, A_1, A_2 are dimensionless parameters, and λ is specified in micrometers. The refractive indices of the Ge substrate determined by these two approaches were in a full agreement in the 2–11.2 μm spectral range. In Fig. 2(a), the obtained optical constants are compared with reference data [36,37] related to bulk Ge samples. Figure 2(b) demonstrates the excellent fitting achieved in the course of the characterization. B260 substrate transparent in the range of 0.4–2.6 μm was used for some samples; its refractive index is specified by the Cauchy formula [Eq. (4)] with $A_0 = 1.51$, $A_1 = 0.52539$, and $A_2 = 6.3281 \cdot 10^{-5}$.

4. CHARACTERIZATION OF THIN FILMS

A. Characterization of ZnS Thin Films

ZnS films were deposited by the evaporation from grains of 1–5 mm size with purity 99.99%; the deposition rate was 1 nm/s. Deposition on B260 substrate (sample ZnS-B260) allowed one to obtain informative features in the VIS–NIR ranges [Fig. 3(c)]. ZnS on Ge substrate (sample ZnS-Ge)

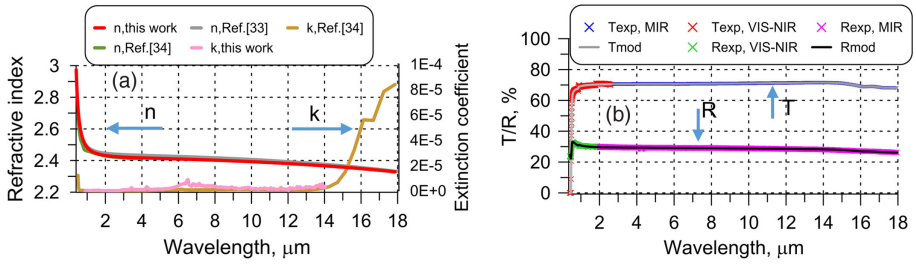

Fig. 1. (a) Determined refractive index of ZnSe substrate and reference data. (b) Fitting of measured transmittance/reflectance data of ZnSe substrate by the model data.

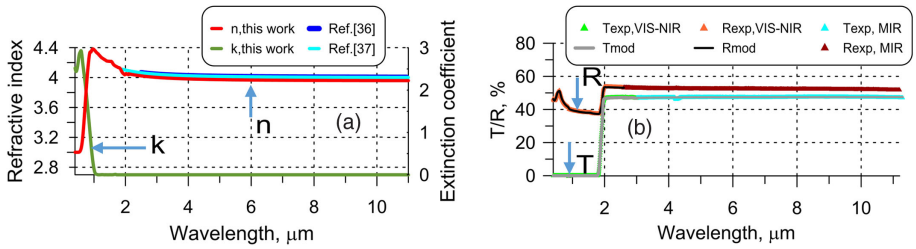

Fig. 2. (a) Determined optical constants of Ge substrate and reference data. (b) Fitting of measured transmittance/reflectance data of Ge substrate by the model data.

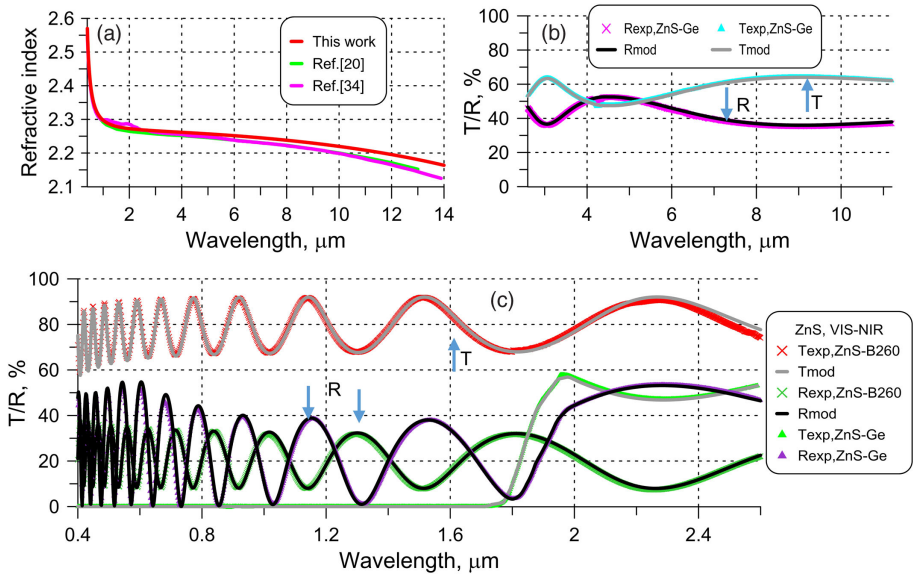

Fig. 3. (a) Determined refractive index of ZnS film and reference data. (b), (c) Fitting of measured transmittance/reflectance data of ZnS-Ge and ZnS-B260 samples by model data in (b) MIR and (c) VIS–NIR.

enabled us to optically characterize the film in the MIR range [Fig. 3(b)].

Taking dispersion of ZnS described by the Sellmeier model from [38] as a starting point, an offset Δ of the refractive index was searched for; the extinction coefficient of the film was described by the exponential model:

$$k(\lambda) = B_0 \cdot \exp\{B_1 \lambda^{-1} + B_2 \lambda\}. \quad \textbf{(5)}$$

The experimental data related to the ZnS-Ge sample was used for the characterization. The DF function [Eq. (1)] was minimized with respect to five parameters Δ, B_0, B_1, B_2, and d. The refractive index offset was $\Delta = 0.012125$; the parameters were found to be equal to $B_0 = 0.03970$, $B_1 = -0.080715$, and $B_2 = -7.074209$. In Fig. 3(a), the determined refractive indices of ZnS are compared with some reference data [34]. Excellent fitting of experimental data in the range of 4–12 μm is demonstrated in Figs. 3(b) and 3(c). In order to verify the results, the determined optical constants of ZnS were fixed, and only the film thickness d was searched for by optimizing the DF function based on the measured data related to the ZnS-B260 sample in the range of 0.4–2.6 μm. The corresponding excellent fitting is shown in Fig. 3(c).

B. Characterization of YbF_3 Thin Films

The YbF_3 evaporation material was initially in granules of 1–3 mm, with purity of 99.99%. The material was preconditioned in order to obtain solid blocks. The deposition rate was 0.3 nm/s. Two YbF_3 thin-film samples, YbF_3-ZnSe-1 and YbF_3-ZnSe-2, with planned thicknesses 2 μm and 0.8 μm on ZnSe substrates were prepared. In both samples, water absorption dips around 3 μm and 6 μm are observed [Fig. 4(b)]. The measurement data points around water absorption peaks were excluded from the optimization process [Eq. (1)]. The extinction coefficient in this spectral range is assumed to be zero. It should be noted that water absorption dips do not affect the phase performance of the laser optical elements (see, for example, [5]).

In the course of optical characterization, the dispersion behavior of the YbF_3 refractive index was described by the Cauchy model [Eq. (4)]; for the extinction coefficient $k(\lambda)$, the non-parametric approach [Eq. (2)] was chosen. Optical constants of YbF_3 obtained from the data related to the YbF_3-ZnSe-1 sample and reference data are shown in Fig. 4(a). Excellent correspondence between measured and model data related to both YbF_3-ZnSe-1 and YbF_3-ZnSe-2 samples is shown in Figs. 4(b) and 4(c). The Cauchy parameters were $A_0 = 1.484489$, $5.4996 \cdot 10^{-5}$, and $2.6266 \cdot 10^{-3}$.

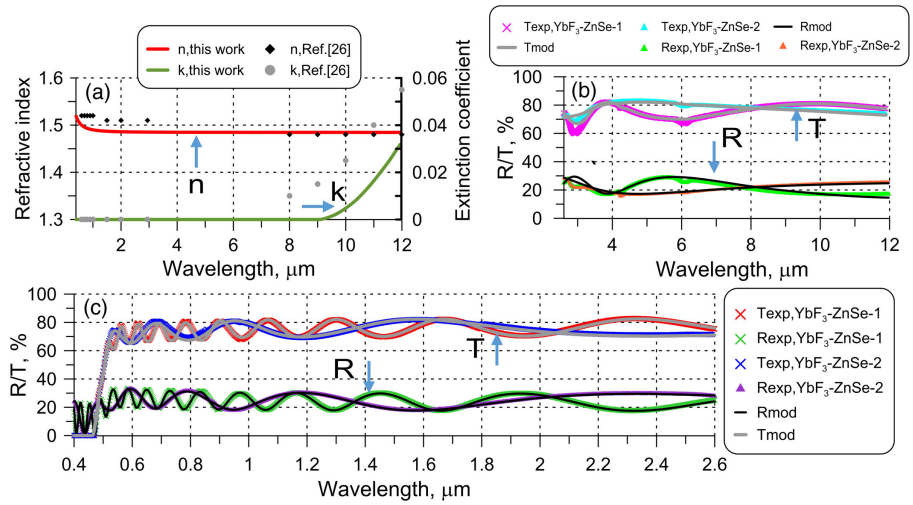

Fig. 4. (a) Determined refractive index of YbF_3 film and reference data. (b), (c) Fitting of measured transmittance/reflectance data of YbF_3-ZnSe-1 and YbF_3-ZnSe-2 samples by model data in (b) MIR and (c) VIS–NIR.

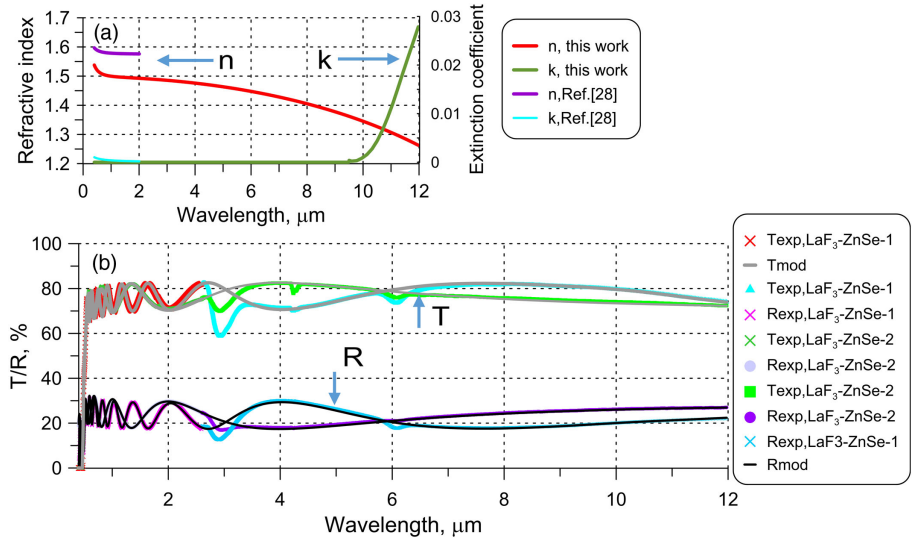

Fig. 5. (a) Determined refractive index of LaF_3 film and reference data. (b) Fitting of measured transmittance/reflectance data of LaF_3-ZnSe-1 and LaF_3-ZnSe-2 samples by model data.

C. Characterization of LaF_3 Thin Films

LaF_3 films were evaporated from grains of 0.7–3.5 mm size with purity of 99.9%; the deposition rate was 0.55 nm/s. Two thin-film samples, LaF_3-ZnSe-1 and LaF3-ZnSe-2, with planned thicknesses of 1.3 μm and 0.65 μm were prepared. Dispersion behavior of the LaF_3 refractive index was described by the Sellmeier model [Eq. (3)], and its extinction coefficient was searched for in the frame of the non-parametric approach [Eq. (2)]. The experimental data from the spectral ranges affected by the water absorption, 2.7–3.4 μm and 5.7–6.5 μm, were excluded from the characterization process. The determined optical constants of LaF_3 film as well as the achieved fitting of the experimental data by model curves corresponding to the LaF_3-ZnSe-1 sample are depicted in Fig. 5. In addition, for the verification of the results, the comparison of model and experimental transmittance data corresponding to the LaF_3-ZnSe-2 sample is shown in Fig. 5. It is seen from Fig. 5 that the determined constants have the same pattern as the data from [28] covering the range up to 2 μm only; the numerical values of the refractive index are lower than in [28].

D. Characterization of Ge Thin Films

The germanium material was initially in granules of 0.7–3.5 mm with purity of 99.999%. The material was melted in order to achieve a dense form. The deposition rate was 0.6 nm/s. Two Ge thin-film samples with planned thicknesses of 0.45 μm and 0.9 μm were produced. In both samples, no water absorption dips were observed (Fig. 7).

Keeping in mind the complicated behavior of Ge optical constants in the VIS–NIR ranges, more informative measurement data was provided. Namely, in order to increase the reliability

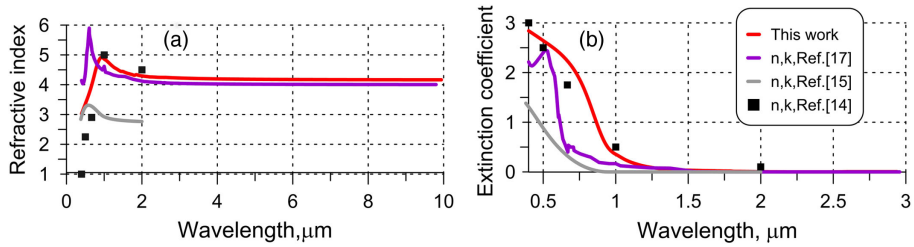

Fig. 6. (a) Determined refractive index and (b) extinction coefficient of Ge thin film and reference data.

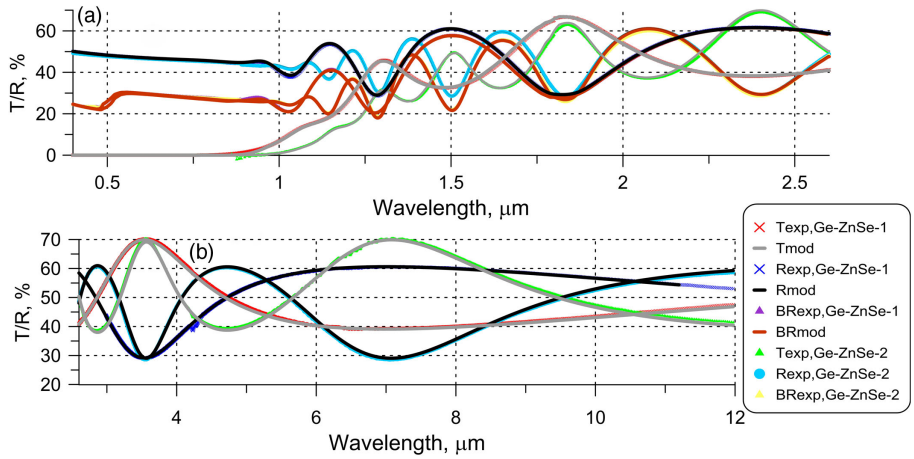

Fig. 7. Comparison of measured transmittance/reflectance data of Ge thin-film samples in (a) VIS–NIR and (b) MIR spectral ranges. BR denotes back side reflection.

of the characterization results, back side reflectance was measured as well [Figs. 7(b) and 7(c)]. To describe the wavelength dependencies $n(\lambda)$, $k(\lambda)$ of Ge thin films, the non-parametric approach [Eq. (2)] was used in the spectral range of 0.4–2 μm (Fig. 6). In the spectral range from 2 to 11 μm, the refractive index of Ge film was described by the Cauchy model. The characterization process was performed for the sample Ge-ZnSe-1. Two obtained wavelength dependencies were merged, and excellent consistence of the dispersion curves in two spectral ranges was observed [Fig. 6(a)]. It is seen from Fig. 6 that the determined n and k wavelength dependencies exhibit the same pattern as in Refs. [14,15,17]; quantitative agreement with the data from [14] is remarkable. In Fig. 7 the achieved excellent fitting of experimental data by model data is shown. For verification purposes, the optical constants found above were fixed and the data related to the sample Ge-ZnSe-2 were processed to find the actual thickness of the second Ge film. The corresponding fitting is presented in Fig. 7.

5. ADHESION, MECHANICAL STRESSES, AND SURFACE ROUGHNESS OF MIR THIN FILMS

The simplest adhesion tape tests, addressed as tests of a "go-no-go" nature [39], were performed. A fresh piece of a kapton tape (1 × 1 cm) was carefully glued on the layer, and then the tape was removed steadily in the direction normal to the coated surface. For each sample, the test was performed several times with intervals of 1–2 months. All produced samples passed the test successfully. All samples were stored in plastic boxes at room temperature without any special precautions. Transmittance/reflectance measurements in the VIS–MIR spectral ranges were repeated several times. The measurements exhibited no additional water absorption and no shifts of spectral curves within 1–2 month intervals.

The mechanical stresses of the thin films were estimated using the well-known Stoney formula [40,41]. For this purpose, thick layers of Ge, ZnS, YbF_3, and LaF_3 were deposited on thin (1 mm) B260 substrates. The radii of curvature of the uncoated and coated substrates were measured using the Dektak 150 Stylus Profiler (Veeco). It was found that Ge and ZnS films exhibit compressive stress with estimated values of (−50) MPa and (−400) MPa, respectively; YbF_3, and LaF_3 films have tensile stresses, which are in agreement with [42]; the estimated values are 140 MPa and 380 MPa, respectively. The accuracy of the estimation is about 10%.

The surface roughness of the MIR thin films and surfaces of two additional uncoated Ge and ZnSe substrates has been measured with an atomic force microscope in non-contact mode. For each material or substrate, at least four different positions were examined. For the evaluation of the results, the software Gwyddion [43] was used. The root-mean-squared (RMS) roughness for the substrates was 1.0 nm for a Ge substrate and 0.6 nm for a ZnSe substrate. For the MIR materials, 3.8 nm for Ge, 4.1 nm for YbF_3, 4.7 nm for LaF_3, and 5.5 nm for ZnS were measured; the accuracy is 1 nm. Figure 8 shows the topography of ZnS and Ge surfaces. While ZnS shows a homogeneous topography, Ge has more impurities that are significant. Overall, the RMS roughness is still lower for Ge

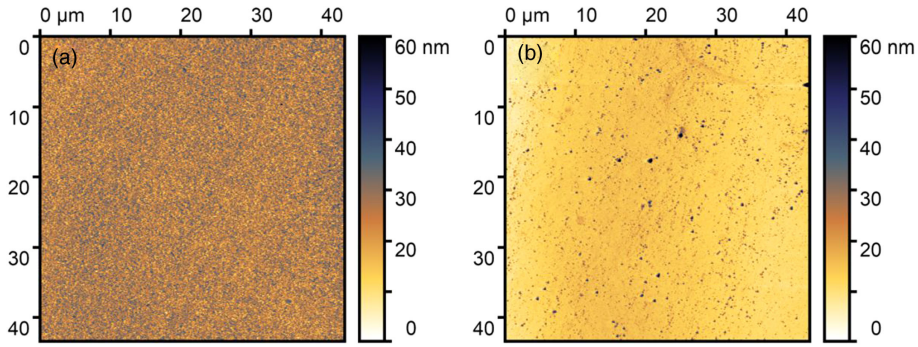

Fig. 8. AFM graphs of surfaces of (a) ZnS and (b) Ge films.

since only certain spots exhibit the maximum peak values. For MIR coatings, all materials have sufficiently low roughness.

6. DISCUSSION OF MATERIALS FOR USE IN LASER-ORIENTED COATINGS

The pairs Ge/LaF_3 and Ge/YbF_3 provide a similar ratio of the refractive index values; LaF_3 is easier in production since it sublimates and does not require melting. On the other hand, the O-H absorption in the LaF_3 layer is more pronounced, and expected stresses are higher, although they can compensate stresses in Ge layers. The combinations ZnS/YbF_3 and ZnS/LaF_3 provide an intermediate ratio of the refractive index values not allowing one to exploit them for the ultra-broadband MIR coatings. At the same time, the combinations ZnS/YbF_3 and ZnS/LaF_3 can be used for NIR–MIR coatings. In order to prevent penetration of water into the multilayer samples, ZnS layers on the top of the layer stack can be used. The well-established pair Ge/ZnS does not raise the water absorption issue, on the one hand, but provides an intermediate ratio of the refractive indices, on the other hand. The thin-film material combination Ge/YbF_3 has the greatest potential for the production of broadband dispersive mirrors operating in the MIR range [5] due to (i) the high contrast of the refractive index values, and (ii) low water absorption of YbF_3 layers. Also, the opposite stresses in high- and low-index layers reduce the resulting stress in Ge/YbF_3 multilayers.

7. CONCLUSIONS

Four thin-film e-beam evaporated materials were carefully characterized: appropriate dispersion models were applied, and optical constants of materials were determined; stresses were estimated. The films exhibit excellent adhesion.

Funding. Munich-Centre for Advanced Photonics.

REFERENCES

1. M. Ebrahim-Zadeh and K. Vodopyanov, "Mid-infrared coherent sources and applications: introduction," J. Opt. Soc. Am. B **33**, MIC1 (2016).
2. M. J. Baker, J. Trevisan, P. Bassan, R. Bhargava, H. J. Butler, K. M. Dorling, P. R. Fielden, S. W. Fogarty, N. J. Fullwood, K. A. Heys, C. Hughes, P. Lasch, P. L. Martin-Hirsch, B. Obinaju, G. D. Sockalingum, J. Sulé-Suso, R. J. Strong, M. J. Walsh, B. R. Wood, P. Gardner, and F. L. Martin, "Using Fourier transform IR spectroscopy to analyze biological materials," Nat. Protoc. **9**, 1771–1791 (2014).
3. P. Baumeister, *Optical Coating Technology* (SPIE Optical Engineering, 2004).
4. F. Habel and V. Pervak, "Dispersive mirror for the mid-infrared spectral range of 9-11.5 µm," Appl. Opt. **56**, C71–C74 (2017).
5. T. Amotchkina, M. Trubetskov, S. A. Hussain, D. Hahner, D. Gerz, M. Huber, W. Schweinberger, I. Pupeza, F. Krausz, and V. Pervak, "Broadband dispersive Ge/YbF_3 mirrors for mid-infrared spectral range," Opt. Lett. **44**, 5210–5213 (2019).
6. J. Zhang, K. Fai Mak, N. Nagl, M. Seidel, D. Bauer, D. Sutter, V. Pervak, F. Krausz, and O. Pronin, "Multi-mW, few-cycle mid-infrared continuum spanning from 500 to 2250 cm^{-1}," Light Sci. Appl. **7**, 17180 (2018).
7. C. Gaida, T. Heuermann, M. Gebhardt, E. Shestaev, T. P. Butler, D. Gerz, N. Lilienfein, P. Sulzer, M. Fischer, R. Holzwarth, A. Leitenstorfer, I. Pupeza, and J. Limpert, "High-power frequency comb at 2 µm wavelength emitted by a Tm-doped fiber laser system," Opt. Lett. **43**, 5178–5181 (2018).
8. M. Seidel, X. Xiao, S. A. Hussain, G. Arisholm, A. Hartung, K. T. Zawilski, P. G. Schunemann, F. Habel, M. Trubetskov, V. Pervak, O. Pronin, and F. Krausz, "Multi-watt, multi-octave, mid-infrared femtosecond source," Sci. Adv. **4**, eaaq1526 (2018).
9. T. P. Butler, D. Gerz, C. Hofer, J. Xu, C. Gaida, T. Heuermann, M. Gebhardt, L. Vamos, W. Schweinberger, J. A. Gessner, T. Siefke, M. Heusinger, U. Zeitner, A. Apolonski, N. Karpowicz, J. Limpert, F. Krausz, and I. Pupeza, "Watt-scale 50 MHz source of single-cycle waveform-stable pulses in the molecular fingerprint region," Opt. Lett. **44**, 1730–1733 (2019).
10. Q. Wang, J. Zhang, A. Kessel, N. Nagl, V. Pervak, O. Pronin, and K. F. Mak, "Broadband mid-infrared coverage (2–17 µm) with few-cycle pulses via cascaded parametric processes," Opt. Lett. **44**, 2566–2569 (2019).
11. E. Fill, "A pellicle coupled optical resonator," in *The European Conference on Lasers and Electro-Optics* (2019).
12. T. Amotchkina, M. Trubetskov, M. Schulz, and V. Pervak, "Comparative study of NIR-MIR beamsplitters based on ZnS/YbF_3 and Ge/YbF_3," Opt. Express **27**, 5557–5569 (2019).
13. Y. Matsuoka, M. P. Semtsiv, S. Peters, and W. Ted Masselink, "Broadband multilayer antireflection coating for quantum cascade laser facets," Opt. Lett. **43**, 4723–4726 (2018).
14. S. Wilbrandt, C. Franke, V. Todorova, O. Stenzel, and N. Kaiser, "Infrared optical constants determination by advanced FTIR techniques," in *Optical Interference Coatings* (OSA, 2016), p. MC.10.
15. A. Ciesielski, L. Skowronski, W. Pacuski, and T. Szoplik, "Permittivity of Ge, Te and Se thin films in the 200–1500 nm spectral range. Predicting the segregation effects in silver," Mater. Sci. Semicond. Process. **81**, 64–67 (2018).
16. J. E. Davey, R. J. Tiernan, T. Pankey, and M. D. Montgomery, "The effect of vacuum-evaporation parameters on the structural, electrical and optical properties of thin germanium films," Solid-State Electron. **6**, 205–216 (1963).

17. E. Palik, *Handbook of Optical Constants of Solids II* (Academic, 1991).
18. M. Friz and F. Waibel, "Coating materials," in *Optical Interference Coatings* (Springer, 2003), pp. 105–130.
19. H. K. Pulker, "Characterization of optical thin films," Appl. Opt. **18**, 1969–1977 (1979).
20. M. Debenham, "Refractive indices of zinc sulfide in the 0.405–13 μm wavelength range," Appl. Opt. **23**, 2238–2239 (1984).
21. C. A. Klein, "Room-temperature dispersion equations for cubic zinc sulfide," Appl. Opt. **25**, 1873–1875 (1986).
22. E. Ritter and R. Hoffmann, "Influence of substrate temperature on the condensation of vacuum evaporated films of MgF_2 and ZnS," J. Vac. Sci. Technol. **6**, 733–736 (1969).
23. Y. Zhang, S. Xiong, W. Huang, and K. Zhang, "Determination of refractive index and thickness of YbF_3 thin films deposited at different bias voltages of APS ion source from spectrophotometric methods," Adv. Opt. Technol. **7**, 33–37 (2018).
24. M. Kennedy, D. Ristau, and H. Niederwald, "Ion beam-assisted deposition of MgF_2 and YbF_3 films," Thin Solid Films **333**, 191–195 (1998).
25. W. Su, B. Li, D. Liu, and F. Zhang, "The determination of infrared optical constants of rare earth fluorides by classical Lorentz oscillator model," J. Phys. Appl. Phys. **40**, 3343–3347 (2007).
26. J. D. Traylor Kruschwitz and W. T. Pawlewicz, "Optical and durability properties of infrared transmitting thin films," Appl. Opt. **36**, 2157–2159 (1997).
27. M. Bischoff, D. Gäbler, N. Kaiser, A. Chuvilin, U. Kaiser, and A. Tünnermann, "Optical and structural properties of LaF_3 thin films," Appl. Opt. **47**, C157–C161 (2008).
28. L. V. Rodríguez-de Marcos, J. I. Larruquert, J. A. Méndez, and J. A. Aznárez, "Self-consistent optical constants of MgF_2, LaF_3, and CeF_3 films," Opt. Mater. Express **7**, 989–1006 (2017).
29. S. F. Pellicori and E. Colton, "Fluoride compounds for IR coatings," Thin Solid Films **209**, 109–115 (1992).
30. O. Stenzel and R. Petrich, "Flexible construction of error functions and their minimization: application to the calculation of optical constants of absorbing or scattering thin-film materials from spectrophotometric data," J. Phys. Appl. Phys. **28**, 978–989 (1995).
31. T. V. Amotchkina, V. Janicki, J. Sancho-Parramon, A. V. Tikhonravov, M. K. Trubetskov, and H. Zorc, "General approach to reliable characterization of thin metal films," Appl. Opt. **50**, 1453–1464 (2011).
32. A. V. Tikhonravov and M. K. Trubetskov, "OptiLayer software," http://www.optilayer.com.
33. J. Connolly, B. diBenedetto, and R. Donadio, "Specifications of raytran material," in *Contemporary Optical Systems and Components Specifications*, R. E. Fischer, ed. (1979), pp. 141–144.
34. M. Querry, *Optical Constants of Minerals and Other Materials from the Millimeter to the Ultraviolet* (1987).
35. T. V. Amotchkina, M. K. Trubetskov, A. V. Tikhonravov, V. Janicki, J. Sancho-Parramon, and H. Zorc, "Comparison of two techniques for reliable characterization of thin metal-dielectric films," Appl. Opt. **50**, 6189–6197 (2011).
36. N. P. Barnes and M. S. Piltch, "Temperature-dependent Sellmeier coefficients and nonlinear optics average power limit for germanium," J. Opt. Soc. Am. **69**, 178–180 (1979).
37. H. H. Li, "Refractive index of silicon and germanium and its wavelength and temperature derivatives," J. Phys. Chem. Ref. Data **9**, 561–658 (1980).
38. B. Tatian, "Fitting refractive-index data with the Sellmeier dispersion formula," Appl. Opt. **23**, 4477–4485 (1984).
39. H. A. Macleod, *Thin-Film Optical Filters*, 4th ed. (Taylor & Francis, 2010).
40. A. E. Ennos, "Stresses developed in optical film coatings," Appl. Opt. **5**, 51–61 (1966).
41. S. Kičas, U. Gimževskis, and S. Melnikas, "Post deposition annealing of IBS mixture coatings for compensation of film induced stress," Opt. Mater. Express **6**, 2236–2243 (2016).
42. E. Fukumoto, T. Aoki, and S. Ogura, "Internal stress properties of fluoride thin films for VUV applications," in *Optical Interference Coatings* (OSA, 2001), p. TuF9.
43. D. Nečas and P. Klapetek, *Gwyddion—Free SPM (AFM, SNOM/NSOM, STM, MFM,. . .) Data Analysis Software* (2019).